BIOCHEMISTRY
including biophysical chemistry & molecular biology
Article

Biochemistry **2010,** *49,* 8937–8943 8937
DOI: 10.1021/bi100600j

Role of Isoleucine-554 in Lithium Binding by the Na^+/Dicarboxylate Cotransporter NaDC1[†]

Ana M. Pajor* and Nina N. Sun

Skaggs School of Pharmacy and Pharmaceutical Sciences, University of California San Diego, La Jolla, California 92093-0718, United States

Received April 19, 2010; Revised Manuscript Received September 14, 2010

ABSTRACT: Sodium-coupled transport of citric acid cycle intermediates, such as succinate and citrate, is mediated by the NaDC1 transporter located on the apical membrane of kidney proximal tubule and small intestine cells. Our previous study showed that transmembrane helix (TM) 11 of NaDC1 is important for sodium and lithium binding, as well as for determining citrate affinity [Kahn and Pajor (1999) *Biochemistry 38*, 6151]. In the present study, 21 amino acids in TM11 and the extracellular loop of NaDC1 were mutated one at a time to cysteine. All of the mutants were well expressed on the plasma membrane, but many of them had decreased transport activity. The G550C, W561C, and L568C mutants were inactive, suggesting that these residues may be critical for function. None of the cysteine mutants was sensitive to inhibition by the membrane-impermeant cysteine reagents, MTSET or MTSES, suggesting that the helix is inaccessible to the extracellular solvent. Although NaDC1 is inhibited by low concentrations of lithium in the presence of sodium, the I554C mutant was stimulated by lithium with a $K_{0.5}$ of 4.8 mM. The I554C mutant also had decreased affinity for sodium. We conclude that TM11 is likely to be an outer helix in NaDC1 that contains several residues critical for transport. Ile-554 in the middle of the helix may be an important determinant of cation affinity and selectivity, in particular the high affinity cation binding site that recognizes lithium.

The Na^+/dicarboxylate cotransporter 1 (NaDC1)[1] is part of a large superfamily of anion transporters called DASS (divalent anion sodium symporters) (*1*). The mammalian members of DASS form the SLC13 family. NaDC1 is found on the plasma membrane of renal proximal tubule and small intestinal cells where it mediates the absorption of citric acid cycle intermediates, such as succinate and citrate (*2*). The transport mechanism involves the ordered binding of three sodium ions, followed by one divalent anion substrate. NaDC1 also interacts with lithium, which appears to compete with sodium at one of the three sodium binding sites producing transport inhibition (*3*). In human patients treated with lithium, there is increased urinary excretion of citric acid cycle intermediates, most likely due to inhibition of renal NaDC1 (*4*).

The current secondary structure model of NaDC1 contains 11 transmembrane helices (TM) with an intracellular N-terminus and an N-glycosylated extracellular C-terminus (*2*). Hydropathy profile analysis suggests that NaDC1 belongs to the ST[3] structural class, which also contains proteins with 11 predicted TM (*5*). There are no crystal structures available for any member of the DASS/SLC13 family, and the only structural information available comes from mutagenesis studies. There is evidence from previous studies that the last transmembrane helix, TM11, and residues in the extracellular C-terminal tail of NaDC1 are functionally important. TM11 was shown in chimera studies to contain residues that determine differences in sodium and citrate affinity, as well as interactions with lithium (*6*). In addition, His-569 on the extracellular C-terminal tail just outside of TM11 is one of two inhibitory binding sites for diethyl pyrocarbonate (DEPC) in NaDC1 (*7*).

In the present study, we performed cysteine-scanning mutagenesis of the outer portion of TM11 and the associated extracellular C-terminal tail. Twenty-one amino acids from Ile-549 to His-569 were mutated one at a time to cysteine. The domain appears to have functional significance because about half of the cysteine mutants had low or no activity despite being well expressed at the plasma membrane. None of the cysteine mutants was affected by treatment with cysteine-specific reagents, suggesting that TM11 is likely to be an outer helix that is inaccessible to the outer solvent. However, I554C, approximately half-way into the helix, appears to interact with cations. The I554C mutant had decreased sodium affinity, and it was stimulated by lithium in the presence of sodium. We conclude that Ile-554 may be an important determinant of cation binding in NaDC1, particularly in the high-affinity cation binding site that accepts lithium.

EXPERIMENTAL PROCEDURES

Site-Directed Mutagenesis. Twenty-one amino acids in the outer portion of TM11 and the associated loop of rbNaDC1 were individually mutated to cysteines using the QuikChange site-directed mutagenesis kit (Stratagene). The parental transporter for this project was the 4N mutant of rabbit NaDC1, containing four endogenous cysteines at the N-terminus (positions 4, 38, 50, and 64) in the pcDNA3.1 vector (Invitrogen). The previous name

[†]This work was supported by National Institutes of Health Grant DK46269 (A.M.P.).

*To whom correspondence should be addressed. E-mail: apajor@ucsd.edu. Tel: 858-822-7806. Fax: 858-822-5591.

[1]Abbreviations: DASS, divalent anion sodium symporter family; DEPC, diethyl pyrocarbonate; h, human; MTSEA-biotin, *N*-biotinaminoethyl methanethiosulfonate; MTSET, [2-(trimethylammonium)ethyl]-methanethiosulfonate; NaDC1, sodium dicarboxylate cotransporter 1; PMSF, phenylmethanesulfonyl fluoride; rb, rabbit; SLC13, solute carrier family 13; TM, transmembrane helix.

Published on Web 09/16/2010

of 4N was 4C(N term) (*8*). NaDC1 requires at least four cysteines for proper processing to the plasma membrane (*8*), and the 4N mutant is not sensitive to membrane-impermeant methanethiosulfonate reagents, such as [2-(trimethylammonium)ethyl]-methanethiosulfonate (MTSET).

Expression of NaDC1 Mutants in COS-7 Cells. COS-7 cells derived from monkey kidney transformed with SV40 (ATCC CRL-1651) were cultured in Dulbecco's modified Eagle's medium containing Glutamax and 25 mM HEPES (Invitrogen, Carlsbad, CA) supplemented with 10% heat-inactivated fetal calf serum, 100 units/mL penicillin and 100 μg/mL streptomycin at 37 °C in 5% CO_2. Cells were plated on collagen-coated plates at 0.6×10^5 cells per well (24 wells) or 1.5×10^5 cells per well (6 wells). Transient transfections with Fugene 6 (Roche) were done the following day at a 9:3 ratio (1.8 μL of Fugene 6 and 0.6 μg of plasmid DNA) for 24-well plates or a 3:1 ratio (3 μL of Fugene 6 and 1 μg of plasmid DNA) for 6-well plates.

Transport Assays. Transport assays were carried out 48 h after transfections as described (*9*, *10*). The sodium buffer contained, in mM, 140 NaCl, 2 KCl, 1 $MgCl_2$, 1 $CaCl_2$, and 10 HEPES, pH adjusted to 7.4 with 1 M Tris. Choline and lithium buffers contained equimolar choline chloride or LiCl, respectively, in place of NaCl. For the assays, each well was washed twice with choline buffer and then incubated with sodium buffer containing [^{14}C]succinate (~50 mCi/mmol, ~20 μM; Moravek) for 30 min at room temperature. The uptakes were stopped, and radioactivity was washed away with four washes of choline buffer. The wash volume was 1 mL (24-well plates) or 3 mL (6 well plates), and the transport buffer volume was 0.25 mL (24-well plates) or 1 mL (6-well plates). Cells were dissolved in 1% SDS, transferred to scintillation vials, and counted. For all experiments, uptakes in vector-transfected cells were subtracted from uptakes in NaDC1 plasmid-transfected cells to correct for background counts.

Kinetic Experiments. For succinate kinetic experiments, 10 min uptakes were measured with increasing concentrations of nonradiolabeled succinate and constant [^{3}H]succinate (50000 mCi/mmol; ViTrax). The [^{3}H]succinate was used for increased specific activity at the higher substrate concentrations. Kinetic constants were calculated by nonlinear regression to the Michaelis–Menten equation. In sodium activation experiments, the rate of [^{14}C]succinate transport was measured in transport buffer containing sodium concentrations between 0 and 140 mM, with NaCl replaced isoosmotically by choline chloride. Kinetic constants were calculated by nonlinear regression to the Hill equation, $v = V_{max}[Na^+]^{n_H}/(K_{Na} + [Na^+])^{n_H}$, where v is the initial rate of succinate uptake, V_{max} is the maximum rate at saturating sodium concentration, $[Na^+]$ is the sodium concentration, K_{Na} is the sodium concentration that produces $(1/2)V_{max}$, and n_H is the Hill coefficient.

Dual-Label Competitive Transport Experiments. The succinate:citrate transport specificity ratio (TSR) was determined using dual-label transport assays in which sodium transport buffer containing both 10 μM [^{3}H]succinate and 20 μM [^{14}C]citrate was added to the cells in 24-well plates, as described previously (*11*). The transport specificity ratio was calculated using $TSR = (v_{succinate}/v_{citrate})([citrate]/[succinate])$, where $v_{succinate}$ and $v_{citrate}$ are the rates of transport of [^{3}H]succinate and [^{14}C]citrate and [citrate] and [succinate] are the concentrations of citrate and succinate (*12*).

Chemical Labeling with MTSET. The NaDC1 mutants expressed in COS-7 cells were preincubated with 250 μL of 1 mM [2-(trimethylammonium)ethyl]methanethiosulfonate (MTSET; Toronto Research Chemicals) in sodium buffer, as described (*10*). The MTSET was weighed out fresh for each experiment, kept on ice, and diluted in buffer just before using. Control groups were preincubated in sodium buffer alone. After 10 min of incubation at room temperature, the cell monolayers were washed three times with sodium buffer and then assayed for succinate transport activity as described above. The transport activity after MTSET treatment was expressed as a percentage of the control group preincubated with buffer only.

Cell Surface Biotinylations. The cell surface expression of NaDC1 mutants in COS-7 cells was determined using the membrane-impermeant reagent, sulfo-NHS-LC-biotin (Pierce), also as described previously (*10*). Briefly, each well of cells in 6-well plates was washed three times with 3 mL of PBS, pH 9, containing 1 mM each Ca^{2+} and Mg^{2+} (PBS/CM) and then incubated for 30 min at room temperature with 0.5 mL of 1.5 mg/mL sulfo-NHS-LC-biotin prepared in PBS/CM. The wells were washed once and then incubated on ice for 20 min with 3 mL of cold quench buffer (PBS/CM with 100 mM glycine). The cells were then treated with 0.5 mL of lysis buffer (1% Triton X-100, 150 mM NaCl, 5 mM EDTA, 20 mM Tris, pH 7.5, supplemented with 10 μg/mL pepstatin, 10 μg/mL leupeptin, and 0.5 mM phenylmethanesulfonyl fluoride) on ice with gentle rocking for 30 min. The lysed cells were transferred to microcentrifuge tubes and pelleted and the supernatants transferred to new tubes. The samples were incubated with 50 μL of immunopure immobilized streptavidin (Pierce) overnight at 4 °C with end-over-end rotation. The next day the beads were washed according to manufacturer's directions, and the eluted samples were used in Western blotting. Blots were incubated with 1:1000 dilution of anti-NaDC-1 antibodies, followed by 1:7500 dilution of peroxidase-conjugated anti-rabbit IgG secondary antibody (Jackson Laboratories). Detection was done using Pierce Supersignal West Pico chemiluminescent substrate and Image Station 4000R (Carestream Scientific).

Labeling of Cysteine Mutants with MTSEA-biotin. The MTSEA-biotin experiments were done as described previously (*10*) except that the NaDC1 mutants were expressed in HeLa cells (ATCC CCL-2) because the background signal was lower. Briefly, cell monolayers were pretreated first with 5 mM dithiothreitol and washed, followed by 1 mM MTSET in sodium transport buffer or sodium buffer alone for 10 min at room temperature. Cells were washed three times with 3 mL of PBS/CM, pH 7.5. A stock solution of 200 mM *N*-biotinylaminoethyl methanethiosulfonate (MTSEA-biotin) (Toronto Research Chemicals) was prepared in dimethyl sulfoxide (DMSO) and was kept dark on ice until use. The MTSEA-biotin solution was further diluted to 0.1 mM with PBS/CM, pH 7.5, just before use. MTSEA-biotin (0.5 mL) was added to each well of a 6-well plate and incubated for 10 min at room temperature with gentle rocking. After the incubation wells were washed three times with 3 mL of PBS/CM, pH 7.5. Lysis buffer with protease inhibitors was added to the plates which were kept on ice with rocking for cell lysis. The remaining steps were identical to those of the cell surface biotinylation procedure. Biotinylated proteins were identified by Western blotting with anti-NaDC1 antibodies.

Statistics. Duplicate or quadruplicate measurements were made for each data point. The experiments were repeated with at least three different batches of transfected cells from different passage numbers. Significant differences between groups were

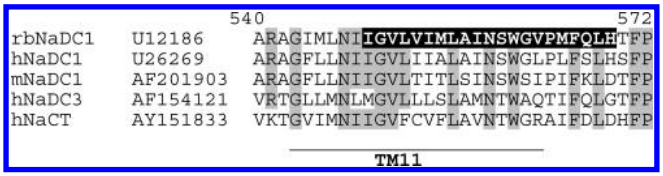

FIGURE 1: Multiple sequence alignment of TM11 and connecting loops in members of the SLC13 family. The amino acid numbering (540−572, shown above the sequences) is based on the rbNaDC1 sequence. The Genbank accession numbers of the nucleotide sequences are shown next to the names. The amino acids mutated in this study (549−569) are in white lettering on a black background, and conserved amino acids are shown with gray backgrounds. The bar below the sequences indicates the putative position of transmembrane domain 11. The helix orientation is from intracellular (left) to extracellular (right).

identified by Student's *t* test or ANOVA with $P < 0.05$. Data are reported as means ± SEM ($n = 3$ or more) or range ($n = 2$).

RESULTS

Cysteine-Scanning Mutagenesis. Twenty-one amino acids in the transmembrane helix (TM) 11 region, between Ile-549 (in the helix) and His-569 (extracellular C-terminal tail), were mutated one at a time to cysteine. The cysteine mutants were made in the 4N mutant of rbNaDC1, containing four endogenous cysteines at the N-terminus. At least 4 out of the 11 endogenous cysteines are required in NaDC1 for proper targeting to the plasma membrane (*8*), and the 4N mutant is not affected by impermeant methanethiosulfonate (MTS) reagents. The location of the mutations and the sequence alignment of the TM11 region from rbNaDC1 and other mammalian members of the SLC13 family are shown in Figure 1. TM11 is approximately located between Gly-543 and Val-563 (*13*−*15*). Our previous study showed that Arg-541 is not required for function (*16*).

Western Blots of Sulfo-NHS-LC Biotinylated Proteins. The cell surface expression of the cysteine mutants was determined by labeling with a membrane-impermeant reagent, sulfo-NHS-LC biotin, that labels extracellular lysine residues. Western blot images are shown in Figure 2, and the summary of results from multiple experiments is shown in Figure 3. All of the mutants were expressed intracellularly and on the plasma membrane. The H569C mutant had the lowest abundance at the cell surface, ~47% of the 4N parental transporter (Figure 3), but the intracellular abundance was similar to that of 4N (not shown). Despite relatively high protein expression on the plasma membrane, more than half of the mutants had impaired transport activity (Figure 3). Gly-550, Trp-561, and Leu-568 are conserved residues (see Figure 1), and the cysteine mutants at these positions had no transport activity. The F566C mutant had measurable activity in only one of four experiments. The I549C, I554C, A557C, G562C, and M565C mutants had activity that was less than 25% of the parental, 4N (Figure 3).

Transport Activity Ratio. Our previous study suggested that residues in the TM11 region may determine differences in citrate affinity in members of the SLC13 family (*6*). Therefore, we tested the cysteine mutants for relative changes in citrate and succinate binding using the transport specificity ratio (TSR) measurement. The TSR compares the relative changes in catalytic efficiency of two substrates, and it is independent of protein expression (*12*). There were no significant differences in TSR between the mutants and parental 4N transporter (results not shown). It should be noted that the TSR is a ratio, and therefore it will only identify changes in binding of one substrate relative to the other.

Effect of Impermeant MTS Reagents. The cysteine mutants were tested for their sensitivity to inhibition by the membrane-impermeant cysteine-specific reagent MTSET. Treatment of the mutants with 1 mM MTSET, which adds a positive charge, did not significantly affect transport activity (results not shown). The T482C mutant of 4N, shown in our previous study to be very sensitive to MTS reagents (*17*), was inhibited more than 90% by the same treatment. T482C was included in every experiment to make sure that the reagent was working properly. There was also no significant effect of MTSES, which adds a negative charge, on the succinate transport activity of the cysteine mutants (not shown).

The lack of response to MTS reagents could be due to inaccessibility of the substituted cysteine or because the labeled residue is not functionally important. Therefore, we tested whether the substituted cysteines at the predicted extracellular surface of the helix and the C-terminal tail could be directly labeled with the cysteine-specific biotinylation reagent, MTSEA-biotin. As shown in Figure 4, the positive control mutant, T482C, was strongly labeled by MTSEA-biotin, and the labeling could be blocked by preincubation with 1 mM MTSET. Two mutants in the putative extracellular C-terminal tail of NaDC1, H569C and Q567C, were also specifically labeled by MTSEA-biotin. It is not clear why L568C was not labeled; the protein abundance of this mutant is high (Figure 2). The P564C and V563C mutants had signals that appeared to be blocked by MTSET, but the signals were very faint, which suggests that these cysteines were not readily accessible from the outside of the cell. Mutants that are predicted to be within the helix, S560C and W561C, were not labeled by MTSEA-biotin.

Lithium Sensitivity of Cysteine Mutants. Our previous study showed that TM11 is important in determining the sensitivity of NaDC1 to inhibition by lithium (*6*). Lithium competes with sodium in NaDC1 at one of the three cation binding sites. Therefore, we tested the effect of 14 mM lithium in the presence of 126 mM sodium on succinate transport by the cysteine mutants. Controls were incubated with buffer containing a combination of 14 mM choline and 126 mM sodium. Treatment of 4N with lithium in the presence of sodium resulted in strong inhibition of succinate transport, with about 50% activity remaining (Figure 5), similar to our previous results with the wild-type rbNaDC1 expressed in *Xenopus* oocytes (*6*). Many of the cysteine mutants also showed similar inhibition by lithium. The I549C, V551C, A557C, I558C, N559C, S560C, and H569C mutants were significantly less inhibited by lithium compared with the response of 4N. In contrast, I554C showed a stimulation of succinate transport activity in the presence of lithium (Figure 5).

The concentration dependence of lithium on succinate transport by 4N and I554C is shown in Figure 6. The experiment was done with 112 mM Na^+ buffer and between 0 and 28 mM Li^+ buffer, with the lithium replaced by choline. The 4N parental transporter showed dose-dependent inhibition of transport, with a maximum inhibition of about 58% (about 42% transport activity remaining). The $K_{0.5}$ was 1.6 mM in the single experiment shown in Figure 6, and the average of five experiments was 1.7 ± 0.4 mM. The I554C mutant was stimulated by increasing concentrations of lithium, to a maximum of about 2.8-fold. The $K_{0.5}$ for activation was 5.2 mM in the single experiment shown in Figure 7, and the mean of three experiments was 4.8 ± 0.7 mM. The transport of succinate in the presence of 140 mM lithium alone was approximately 2.4% of the activity in sodium

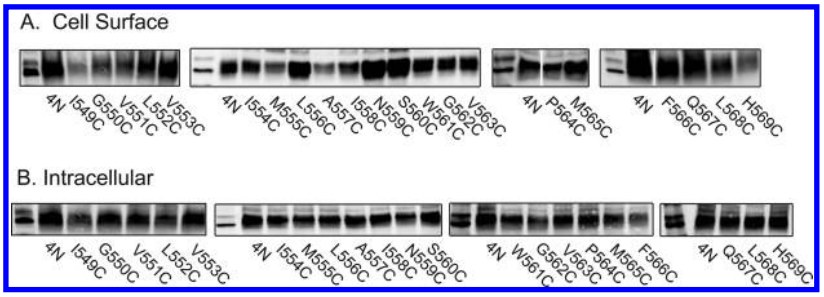

FIGURE 2: Western blots of cell surface (A) and intracellular (B) protein expression. COS-7 cells expressing NaDC1 mutants were treated with sulfo-NHS-LC-biotin, followed by streptavidin−agarose beads. The control for each biotinylation experiment was the parental transporter, 4N, containing four endogenous cysteines at the N-terminus. The first lane in each blot contains the chemiluminescent size standards, MagicMark XP, and the two bands shown are 50 and 60 kDa. The blots were probed with anti-NaDC1 polyclonal antibodies at 1:1000 dilution. Single representative blots are shown, and some lanes after 4N (shown as a gap) have been omitted from the third and fourth blots in panel A.

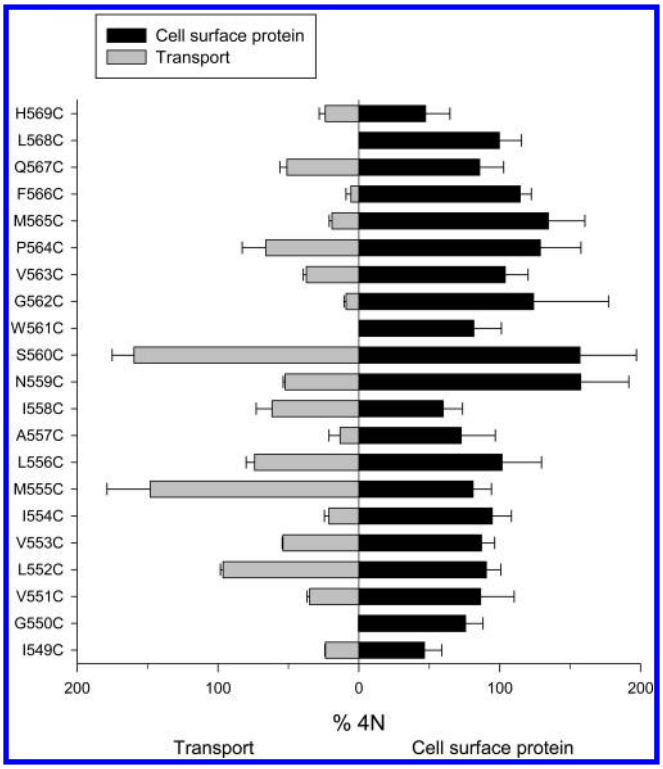

FIGURE 3: Summary of protein expression and transport activity of the cysteine mutants. Left side of figure: Succinate transport activity of cysteine mutants expressed in COS-7 cells. Uptake assays were conducted for 30 min in the presence of 140 mM Na^+ and 20 μM [^{14}C]succinate. Mutants with activity less than 20% of the 4N control were assayed in 6-well plates. Activity is expressed as a percentage of the activity in the 4N control (measured in the same type of plates). Right side of figure: Summary of cell surface protein expression determined by quantitating the intensity of protein bands in Western blots, including the ones shown in Figure 2. The bars represent means ± SEM, n = 3−4 separate experiments.

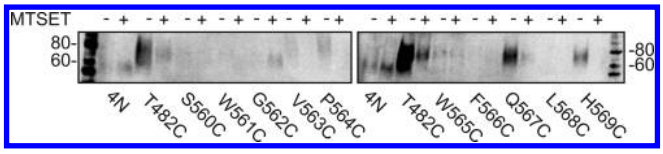

FIGURE 4: Labeling of cysteine-substituted mutants with MTSEA-biotin. The NaDC1 cysteine mutants and a mutant shown previously to be sensitive to MTSET, T482C (*17*), were pretreated for 10 min with 1 mM MTSET (+) or sodium buffer (−) followed by chemical labeling with MTSEA-biotin. The biotinylated samples were transferred to Western blots as described in Experimental Procedures. The chemiluminescent size standards, MagicMark XP, are shown on each blot, and the two bands at 60 and 80 kDa are labeled. The blots were probed with anti-NaDC1 polyclonal antibodies at 1:1000 dilution.

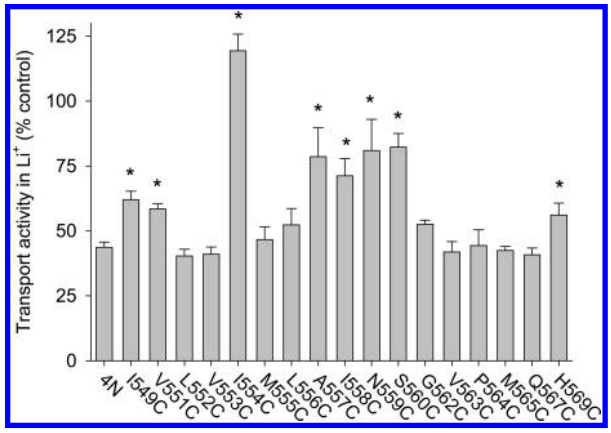

FIGURE 5: Effect of lithium on succinate transport by cysteine mutants. Succinate transport activity was measured in transport buffer containing 126 mM NaCl together with either 14 mM choline chloride (control) or 14 mM LiCl. The transport activity in lithium is expressed as a percentage of the activity in choline. Most of the mutants were inhibited by lithium, with only about 50% activity remaining compared with the choline chloride control. The succinate transport activity of some of the mutants was less inhibited compared with 4N, or significantly stimulated by lithium, shown by asterisks ($P < 0.05$). The bars represent means ± SEM, n = 3−5 (mutants) or 13 (4N) separate experiments.

in I554C and approximately 4% in 4N (not shown). Lithium can replace sodium to support succinate transport by rbNaDC1, but the K_m for succinate is much larger than in sodium (~3 mM in Li^+ vs 0.2 mM in Na^+) (*3*).

Characterization of I554C Mutant. Succinate kinetics of the 4N and I554C mutants were compared. The mean succinate K_m value for 4N was 51 ± 8 μM (n = 4 experiments). The single experiment shown in Figure 7A had a K_m value of 52 μM. The 4N K_m value was similar to the succinate K_m for wild-type rbNaDC1, 70 ± 7 μM (n = 2; not shown). The V_{max} values were 52 ± 20 pmol/min per well (4N, n = 4) and 105 ± 28 pmol/min per well (rbNaDC1, n = 2). The protein expression of the wild-type rbNaDC1 is greater than that of the 4N mutant (*8*). The succinate K_m in I554C was 146 ± 20 μM (n = 4), significantly higher than that of the 4N mutant. The single experiment shown in Figure 7A had a K_m value of 142 μM for I554C. The succinate V_{max} for I554C was 26 ± 2 pmol/min per well (n = 4), not significantly different from the 4N mutant.

Sodium activation curves for I554C and 4N are shown in Figure 7B. The K_{Na} value for I554C was 134 mM in the experiment shown in Figure 7B, which is only an estimate because the

highest sodium concentration that could be tested was 140 mM. In four experiments, the mean estimated K_{Na} for I554C was 155 ± 26 mM, and the mean Hill coefficient was 2.49 ± 0.18. 4N had a K_{Na} value of 60 mM (experiment shown in Figure 7B) and, in a second experiment, a K_{Na} of 86 mM. The Hill coefficients for 4N were 2.85 (Figure 7B) and 1.87. Two experiments with wild-type rbNaDC1 expressed in COS-7 cells had K_{Na} values of 45 and 32 mM, similar to our previous results (*18*).

DISCUSSION

The current secondary structure model of NaDC1 places TM11 between amino acids 543 and 563, with an inside (Gly-543) to outside (Val-563) orientation (Figure 8A). The N-glycosylation site is located at the carboxyl-terminal tail at Asn-576 (*19*). The present study, a cysteine scan of the outer portion of TM11 and the extracellular C-terminal tail, was conducted to identify the role of this region in the function of NaDC1. Twenty-one amino acids between positions 549 and 569 were individually mutated to cysteine. However, most of the mutants had very low succinate transport activity, with less than 50% of the activity of the 4N mutant. Despite the decreased activity, there was no change in the transport specificity ratio that measures substrate selectivity between succinate and citrate. Three of the mutated residues, Gly-550, Trp-561, and Leu-568, are likely to be critical for transport because the mutant proteins had no activity although they were correctly targeted to the plasma membrane. Within TM11, many of the mutants with low activity or increased sensitivity to lithium appeared to be located on one face of the helix (Figure 8B).

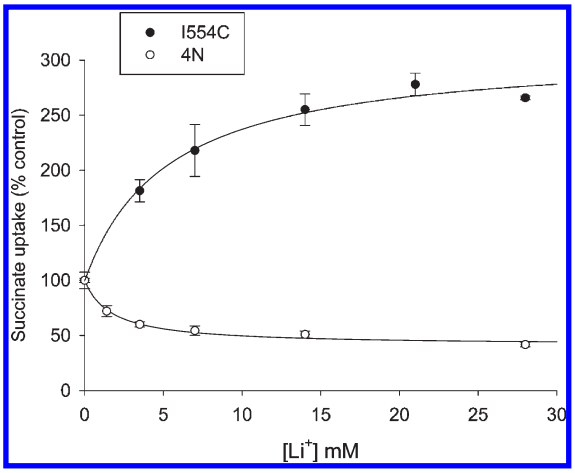

FIGURE 6: Effect of LiCl on I554C and 4N mutants of NaDC1. The transport of [^{14}C]succinate (20 μM) was measured in 112 mM Na^+-transport buffer with between 0 and 28 mM LiCl (the LiCl was replaced by choline chloride). The uptake activity in LiCl was expressed as a percentage of the activity in 28 mM choline chloride (control). In the experiment shown here, the $K_{0.5}$ for Li was 5.2 mM (activation of I554C) and 1.6 mM (inhibition of 4N). The data represent means ± SEM, $n = 4$ replicate points from a single experiment.

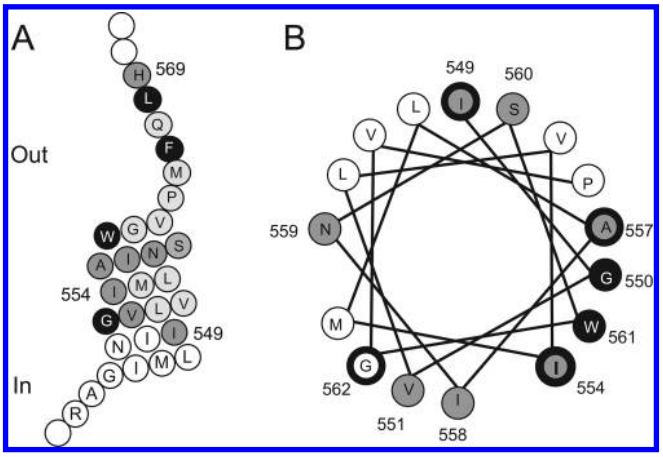

FIGURE 8: Summary of results of cysteine scan. (A) Model of TM11 and C-terminal tail showing the residues between Ile-549 and His-569 that were mutated in this study. The outside of the cell is at the top. Amino acids shaded in black represent inactive mutants (or nearly inactive in the case of F566C), and those shaded in dark gray represent mutants that were affected by lithium. (B) Helical wheel projection of the residues mutated in TM11. Amino acids shaded in black represent inactive mutants, and those shaded in dark gray represent mutants that were affected by lithium. Circles with thicker outlines represent mutants within the helix with less than 25% activity relative to 4N.

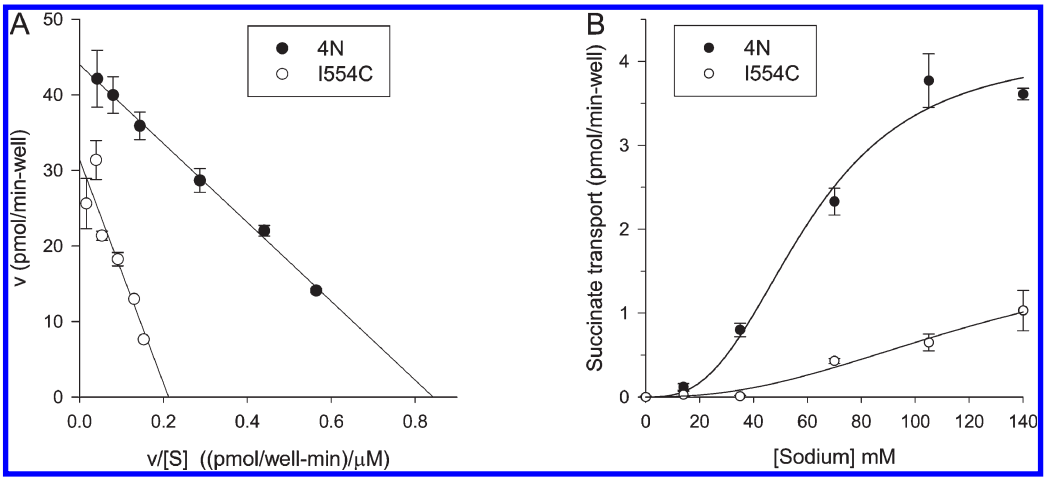

FIGURE 7: Succinate and sodium kinetic properties of the 4N and I554C mutants of rbNaDC1. (A) Succinate kinetics. The initial rate of [^{3}H]succinate transport (v), in pmol/min per well, was measured at increasing succinate concentrations [S], in μM. The data are shown as an Eadie−Hofstee plot. The kinetic constants for 4N were 52 μM (K_m) and 44 pmol/min per well (V_{max}) and for I554C 142 μM (K_m) and 31 pmol/min per well (V_{max}). The data represent means ± SEM, $n = 4$ replicate points from a single experiment. (B) Sodium activation of succinate transport. [^{14}C]Succinate transport (20 μM) was measured in transport buffer containing 0−140 mM NaCl (replaced by choline chloride). The data were fitted to the Hill equation, and the kinetic constants were as follows: 4N, K_{Na} 62 mM, V_{max} 4.3 pmol/min per well, n_H 2.76; I554C, K_{Na} 197 mM, V_{max} 11 pmol/min per well, n_H 2.25. The data represent means ± SEM, $n = 4$ replicate points from a single experiment.

None of the cysteine mutants in the current study was sensitive to chemical modification by membrane-impermeant cysteine-specific reagents, such as MTSET. Two of the mutants, H569C and Q567C, were labeled directly by MTSEA-biotin, suggesting that the modification by MTSET at these positions is not detrimental to function. The other mutants tested did not show labeling by MTSEA-biotin. Therefore, it is likely that most of the residues mutated in this study are not accessible to the outside of the cell. In other studies of transporters, insensitivity to MTS reagents is generally a sign of an outer helix in contact with the lipid bilayer. For example, cysteine-scanning mutagenesis of the lactose permease identified TM III, VI, IX, and XII as outer helices because of a lack of reactivity with cysteine reagents (*20*). This was verified in the crystal structure (*21*). Similarly, several TM in the GLUT1 glucose transporter are predicted to be outer helices that are not accessible to the outside solvent. Some of the helices have functional roles; for example, TM9 is predicted to stabilize the inner helices that form the substrate binding site (*22*). In contrast, TM6 of GLUT1, also predicted to be an outer helix, contains amino acids that are important for the transport function (*23*). Therefore, it is very likely that TM11 in NaDC1 is an outer helix that also contains functionally important residues.

Mutation of His-569 to cysteine resulted in a decrease in cell surface protein expression and a corresponding decrease in succinate transport activity but no significant changes in substrate selectivity. The H569C mutant had a modest increase in lithium sensitivity. It was interesting that the H569C mutant was not affected by chemical modification with MTSET or MTSES, despite labeling by MTSEA-biotin. In our previous study, His-569 and His-153 of NaDC1 were shown to mediate diethyl pyrocarbonate (DEPC) dependent inhibition of succinate transport (*7*). It is possible that structural differences between DEPC and the MTS reagents are responsible for the differences in functional effects.

Of the 21 mutants in the present study, I554C appeared to have the greatest functional changes. The I554C mutant had low transport activity, without much of a change in protein expression. The apparent sodium affinity was reduced in the I554C mutant, with an estimated $K_{Na} \sim 155$ mM compared with 73 mM for 4N. The NaDC1 transport cycle involves cooperative, ordered binding of three sodium ions, followed by a divalent anion substrate (*24*, *25*). The binding of sodium results in an increase in the substrate affinity, shown by a decreased succinate K_m. Although I554C had an increased K_m for succinate of about 146 μM, compared with 51 μM in the parental 4N transporter, the decrease in sodium affinity could also account for this change in K_m. It was not possible to saturate the mutant transporter with sodium at the highest concentration used in our study, 140 mM.

One of the three cation binding sites in NaDC1 binds lithium with high affinity (*3*), although lithium binding does not appear to produce the optimal conformational change in the protein. Transport of succinate in the presence of both lithium and sodium is inhibited. Under voltage clamp conditions and high substrate concentrations, lithium can substitute for sodium in rbNaDC1, but the succinate K_m is increased by about 10-fold (*3*). Lithium behaves as a mixed-type inhibitor (*26*), with a decrease in V_{max} and an increase in K_m for succinate. In the present study, the 4N parental transporter was inhibited about 55% by 14 mM lithium in the presence of 126 mM sodium. In contrast, I554C had transport stimulation under the same conditions. The stimulation by lithium was greater than would be expected by only replacing sodium, and lithium by itself did not substitute well for sodium in I554C. Interestingly, the human Na^+/citrate transporter, NaCT (SLC13A5), exhibits stimulation of transport in the presence of lithium with a mixed-type inhibition involving a decrease in both K_m and V_{max} (*27*). NaCT contains a Val in place of Ile-554 but a Cys in place of Ile-553 (Figure 1).

The GAT-1 GABA transporter is a member of the Na^+/Cl^-/neurotransmitter transporter family, with a model based on the structure of the bacterial homologue LeuT (*28*). GAT-1 interacts with lithium at one of the two sodium binding sites, although the lithium binding affinity is quite low. For example, the combination of 50 mM Li^+ and 100 mM Na^+ does not reduce transport activity in GAT-1 (*29*). Sodium binding sites in this family of transporters are formed by direct contact with oxygen atoms, but some of the oxygens come from backbone carbonyls from unwound portions of TM1 and TM6 rather than from amino acid side chains. The effect of mutations of Asp-395 in GAT-1, which is thought to mediate lithium binding, appears to be both direct, through the loss of a coordinating residue, and indirect, through the movement of another residue into the cation binding site (*30*). Although NaDC1 is not structurally related to GAT-1, it is likely that the effect of mutations in NaDC1 will be similar in producing functional effects either directly on a cation/substrate binding site or indirectly through alterations in helix packing.

In conclusion, this study involved a cysteine scan of the outer portion of TM11 and the associated loop of NaDC1, from Ile-549 to His-569. This portion of the helix and associated loop may be important for function or helix packing because most of the mutants had decreased transport activity despite high expression on the plasma membrane. However, none of the mutants showed a change in function after labeling with membrane-impermeant MTS reagents, suggesting that TM11 in NaDC1 is likely to be an outer helix. Ile-554 was found to be important in determining sodium affinity, as well as lithium sensitivity. The I554C mutant was stimulated by lithium. Therefore, Ile-554 may be an important determinant of cation binding in NaDC1, particularly in the high-affinity cation binding site that accepts lithium.

ACKNOWLEDGMENT

We thank Alva Leung and Jeffrey Young for help in making solutions and Richard Jensen for technical assistance during the initial stages of this project.

REFERENCES

1. Saier, M. H. (1999) A functional phylogenetic system for the classification of transport proteins. *J. Cell Biochem. Suppl.* 32−33, 84–94.
2. Pajor, A. M. (2006) Molecular properties of the SLC13 family of dicarboxylate and sulfate transporters. *Pfluegers Arch. 451*, 597–605.
3. Pajor, A. M., Hirayama, B. A., and Loo, D. D. F. (1998) Sodium and lithium interactions with the Na^+/dicarboxylate cotransporter. *J. Biol. Chem. 273*, 18923–18929.
4. Bond, P. A., Jenner, F. A., Lee, C. R., Lenton, E., Pollitt, R. J., and Sampson, G. A. (1972) The effect of lithium salts on the urinary excretion of α-oxoglutarate in man. *Br. J. Pharmacol. 46*, 116–123.
5. Lolkema, J. S., and Slotboom, D. J. (2003) Classification of 29 families of secondary transport proteins into a single structural class using hydropathy profile analysis. *J. Mol. Biol. 327*, 901–909.
6. Kahn, E. S., and Pajor, A. M. (1999) Determinants of substrate and cation affinities in the Na^+/dicarboxylate cotransporter. *Biochemistry 38*, 6151–6156.
7. Pajor, A. M., Sun, N., and Valmonte, H. G. (1998) Mutational analysis of histidines in the Na^+/dicarboxylate cotransporter, NaDC-1264. *Biochem. J. 331*, 257–264.

8. Pajor, A. M., Krajewski, S. J., Sun, N., and Gangula, R. (1999) Cysteine residues in the Na^+/dicarboxylate cotransporter, NaDC-1. *Biochem. J. 344*, 205–209.
9. Weerachayaphorn, J., and Pajor, A. M. (2008) Threonine-509 is a determinant of apparent affinity for both substrate and cations in the human Na^+/dicarboxylate cotransporter. *Biochemistry 47*, 1087–1093.
10. Pajor, A. M., and Randolph, K. M. (2005) Conformationally sensitive residues in extracellular loop 5 of the Na^+/dicarboxylate co-transporter. *J. Biol. Chem. 280*, 18728–18735.
11. Oshiro, N., King, S. C., and Pajor, A. M. (2006) Transmembrane helices 3 and 4 are involved in substrate recognition by the Na^+/dicarboxylate cotransporter, NaDC1. *Biochemistry 45*, 2302–2310.
12. King, S. C. (2004) The "transport specificity ratio": a structure-function tool to search the protein fold for loci that control transition state stability in membrane transport catalysis. *BMC Biochem. 5*, 16.
13. Rost, B., Yachdav, G., and Liu, J. (2004) The PredictProtein server. *Nucleic Acids Res. 32*, W321–W326.
14. Bryson, K., McGuffin, L. J., Marsden, R. L., Ward, J. J., Sodhi, J. S., and Jones, D. T. (2005) Protein structure prediction servers at University College London. *Nucleic Acids Res. 33*, W36–W38.
15. Arai, M., Mitsuke, H., Ikeda, M., Xia, J. X., Kikuchi, T., Satake, M., and Shimizu, T. (2004) ConPred II: a consensus prediction method for obtaining transmembrane topology models with high reliability. *Nucleic Acids Res. 32*, W390–W393.
16. Pajor, A. M., Kahn, E. S., and Gangula, R. (2000) Role of cationic amino acids in the Na/dicarboxylate co-transporter, NaDC-1. *Biochem. J. 350*, 677–683.
17. Pajor, A. M. (2001) Conformationally-sensitive residues in transmembrane domain 9 of the Na^+/dicarboxylate cotransporter. *J. Biol. Chem. 276*, 29961–29968.
18. Pajor, A. M., and Sun, N. (1996) Functional differences between rabbit and human Na^+-dicarboxylate cotransporters, NaDC-1 and hNaDC-1. *Am. J. Physiol. Renal Physiol. 271*, F1093–F1099.
19. Pajor, A. M., and Sun, N. (1996) Characterization of the rabbit renal Na^+/dicarboxylate cotransporter using anti-fusion protein antibodies. *Am. J. Physiol. Cell Physiol. 271*, C1808–C1816.
20. Frillingos, S., Sahin-Toth, M., Wu, J., and Kaback, H. R. (1998) Cys-scanning mutagenesis: a novel approach to structure-function relationships in polytopic membrane proteins. *FASEB J. 12*, 1281–1299.
21. Abramson, J., Smirnova, I., Kasho, V., Verner, G., Kaback, H. R., and Iwata, S. (2003) Structure and mechanism of the lactose permease of *Escherichia coli*. *Science 301*, 610–615.
22. Mueckler, M., and Makepeace, C. (2009) Model of the exofacial substrate-binding site and helical folding of the human Glut1 glucose transporter based on scanning mutagenesis. *Biochemistry 48*, 5934–5942.
23. Mueckler, M., and Makepeace, C. (2008) Transmembrane segment 6 of the Glut1 glucose transporter is an outer helix and contains amino acid side chains essential for transport activity. *J. Biol. Chem. 283*, 11550–11555.
24. Yao, X., and Pajor, A. M. (2000) The transport properties of the human renal Na^+/dicarboxylate cotransporter under voltage clamp conditions. *Am. J. Physiol.* (*Renal Fluid Electrolyte Physiol.*) *279*, F54–F64.
25. Wright, S. H., Hirayama, B., Kaunitz, J. D., Kippen, I., and Wright, E. M. (1983) Kinetics of sodium succinate cotransport across renal brush-border membranes. *J. Biol. Chem. 258*, 5456–5462.
26. Segel, I. H. (1975) Enzyme kinetics, John Wiley and Sons, New York.
27. Inoue, K., Zhuang, L., Maddox, D. M., Smith, S. B., and Ganapathy, V. (2003) Human sodium-coupled citrate transporter, the orthologue of *Drosophila Indy*, as a novel target for lithium action. *Biochem. J. 374*, 21–26.
28. Yamashita, A., Singh, S. K., Kawate, T., Jin, Y., and Gouaux, E. (2005) Crystal structure of a bacterial homologue of Na^+/Cl^--dependent neurotransmitter transporters. *Nature 437*, 215–223.
29. Grunewald, M., and Kanner, B. (1995) Conformational changes monitored on the glutamate transporter GLT-1 indicate the existence of two neurotransmitter-bound states. *J. Biol. Chem. 270*, 17017–17024.
30. Zhou, Y., Zomot, E., and Kanner, B. I. (2006) Identification of a lithium interaction site in the gamma-aminobutyric acid (GABA) transporter GAT-1. *J. Biol. Chem. 281*, 22092–22099.